Supporting Information

A Portable Near-Infrared Aptasensor Platform for Derivatization-Assisted On-Site Analysis of Acrylamide in Food Samples

Lingli Bu[1], Meixing Liu[1], Qihang Yang[5], Xinkai Li[5], Minglei Li[5], Luyao Li[1*], Song Wang[4*], Sheng Lei[3*], Jiaheng Zhang[2*]

[1] Henan Linker Technology Key Laboratory, College of Advanced Interdisciplinary Science and Technology (CAIST), Henan University of Technology, Zhengzhou 450001, China.

[2] College of Chemistry, Zhengzhou University, Zhengzhou 450001, China

[3] Department of Clinical Laboratory, The First Affiliated Hospital of Guangzhou Medical University, Guangzhou Medical University, Guangzhou, Guangdong 510120, China.

[4] Hubei Yangtze Memory Laboratories, Wuhan 430205, China

[5] China Tobacco Guangdong Industrial Co., Ltd., Guangzhou, Guangdong 510630, China

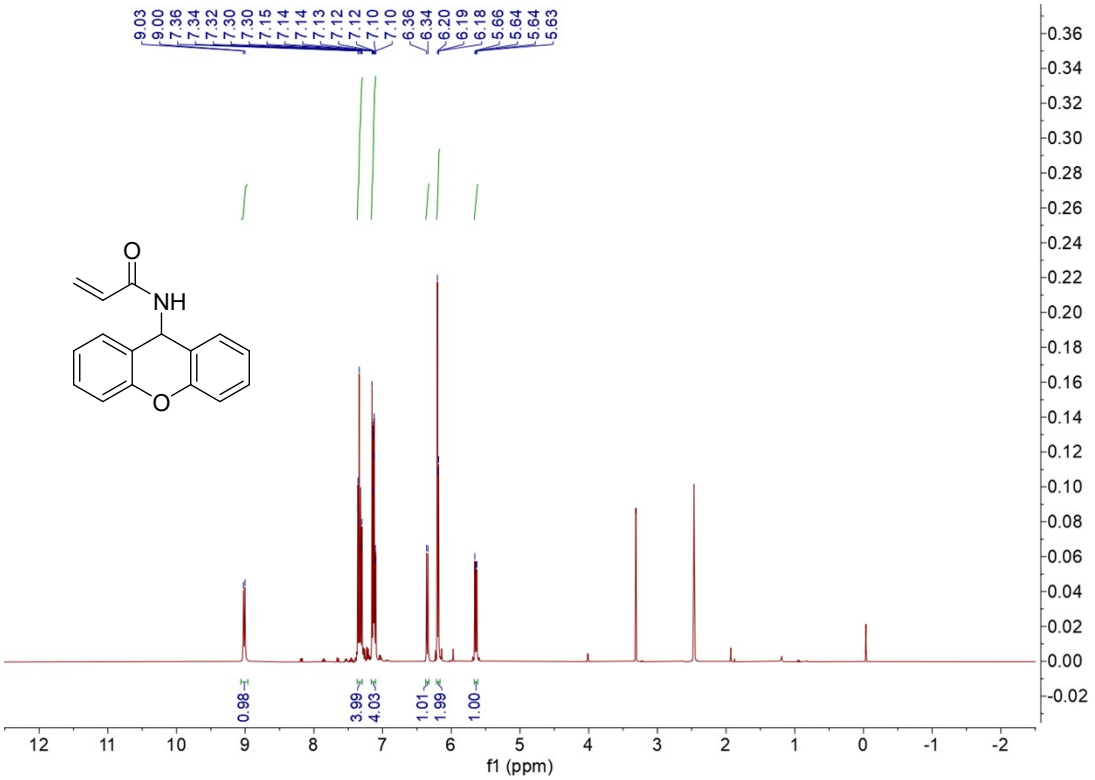

FigureS1 NMR spectra of XAA.^{1}H NMR (400 MHz, DMSO-d_6) δ 9.01 (d, J = 8.7 Hz, 1H), 7.37 – 7.30 (m, 4H), 7.16 – 7.10 (m, 4H), 6.35 (d, J = 8.7 Hz, 1H), 6.21 – 6.16 (m, 2H), 5.64 (dd, J = 7.4, 4.9 Hz, 1H).

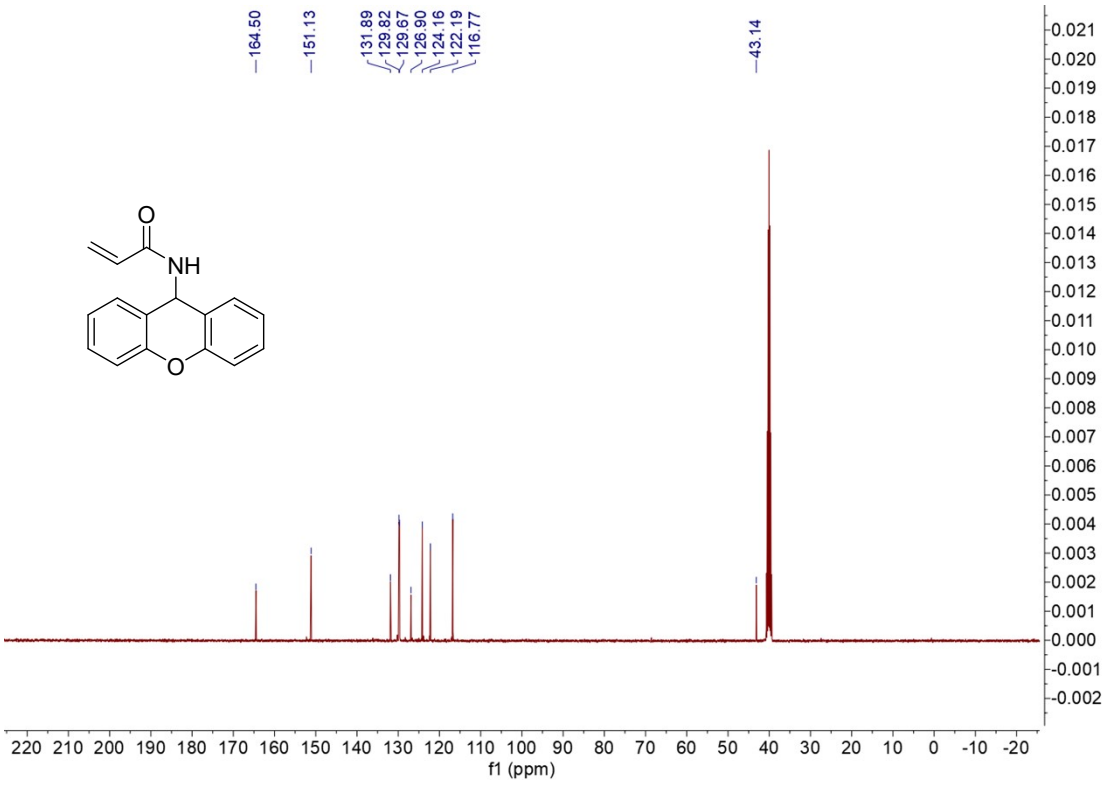

FigureS2 NMR spectra of XAA.^{13}C NMR (101 MHz, DMSO-d_6) δ 164.50, 151.13, 131.89, 129.82, 129.67, 126.90, 124.16, 122.19, 116.77, 43.14.

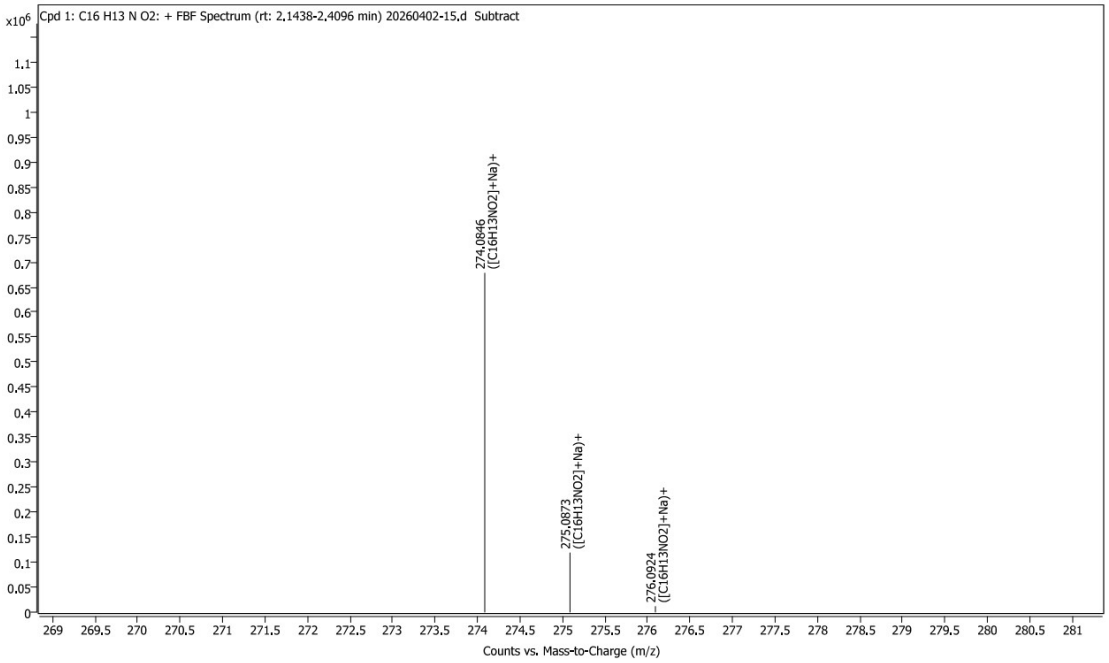

32

33 **FigureS3** HRMS (ESI) spectrum of XAA.

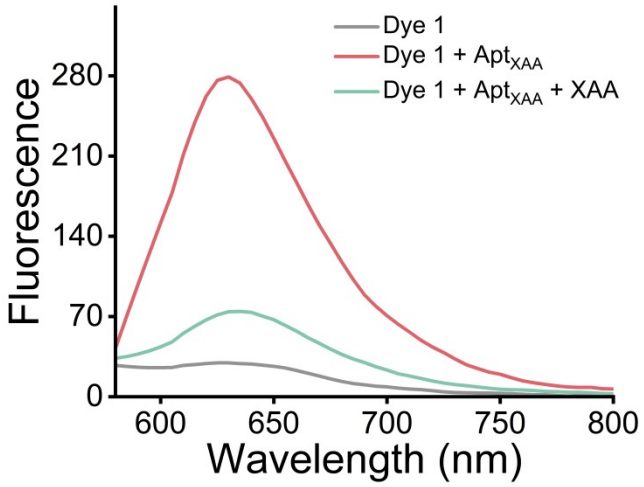

34

35 **Fig. S4** Fluorescence spectra (λ_{ex} = 540 nm) of Solvent Violet 8 (10 μM) upon binding

36 to Apt_{XAA} (5 μM) and subsequent competition with XAA (50 μM) in HEPES buffer.

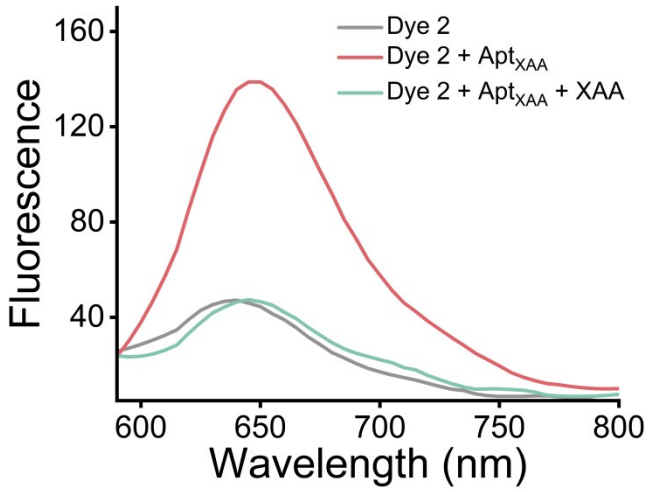

Fig. S5 Fluorescence spectra (λ_{ex} = 550 nm) of Ethyl Violet (10 μM) upon binding to Apt_{XAA} (5 μM) and subsequent competition with XAA (50 μM) in HEPES buffer.

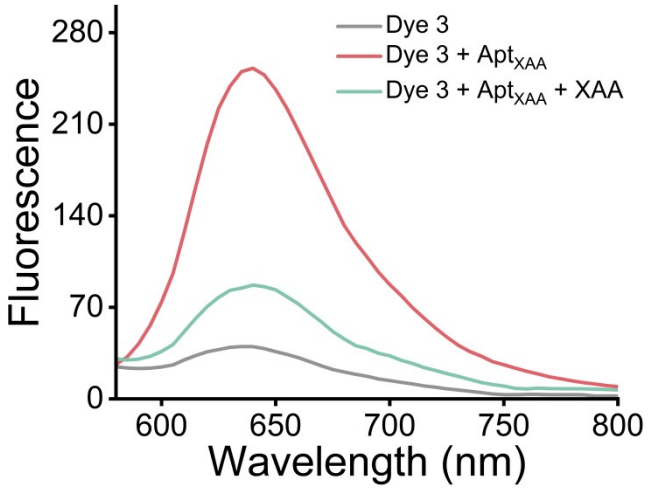

Fig. S6 Fluorescence spectra (λ_{ex} = 540 nm) of Crystal Violet (10 μM) upon binding to Apt_{XAA} (5 μM) and subsequent competition with XAA (50 μM) in HEPES buffer.

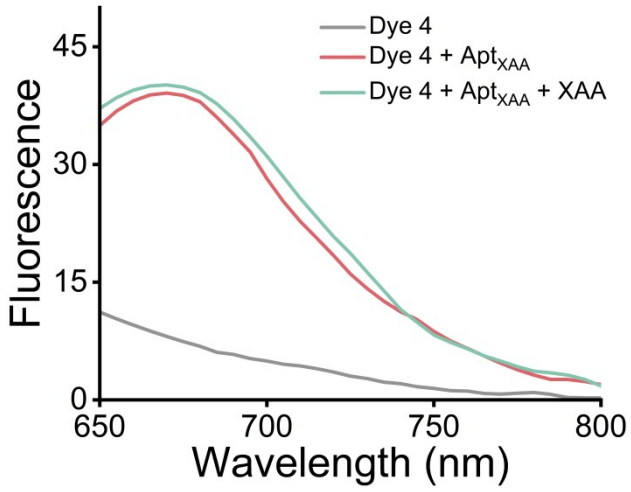

Fig. S7 Fluorescence spectra (λ_{ex} = 600 nm) of Methyl Green (10 μM) upon binding to Apt_{XAA} (5 μM) and subsequent competition with XAA (50 μM) in HEPES buffer.

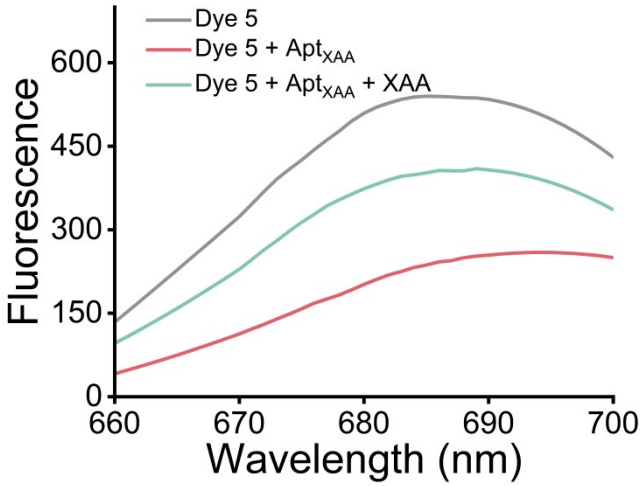

Fig. S8 Fluorescence spectra (λ_{ex} = 600 nm) of Basic Blue 11 (10 μM) upon binding to Apt_{XAA} (5 μM) and subsequent competition with XAA (50 μM) in HEPES buffer.

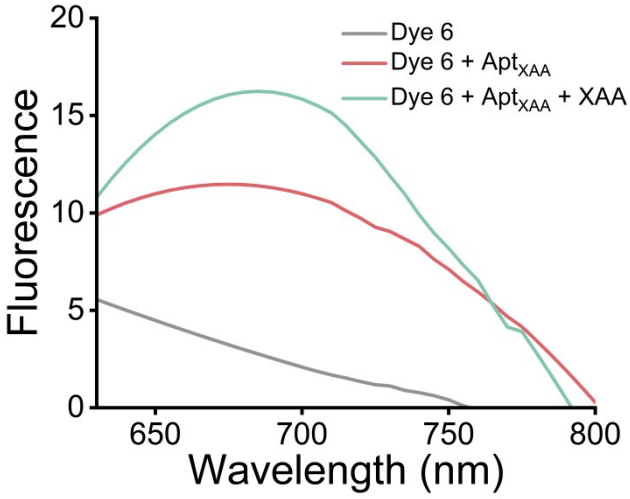

Fig. S9 Fluorescence spectra (λ_{ex} = 585 nm) of Basic Blue 26 (10 μM) upon binding to Apt_{XAA} (5 μM) and subsequent competition with XAA (50 μM) in HEPES buffer.

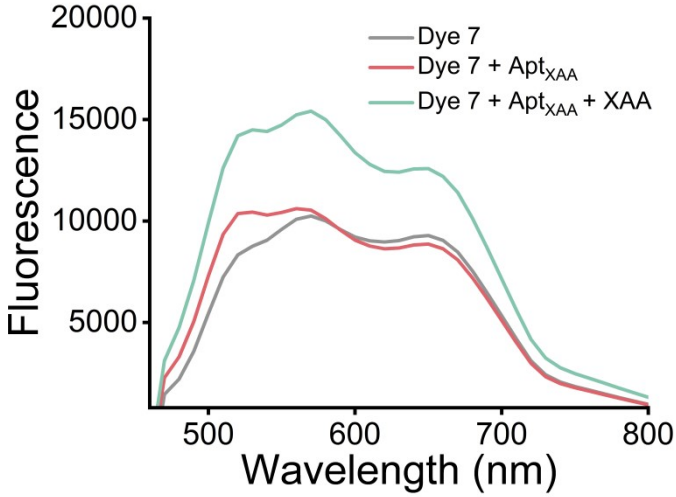

Fig. S10 Fluorescence spectra (λ_{ex} = 400 nm) of Basic Coumarin 6 (10 μM) upon binding to Apt_{XAA} (5 μM) and subsequent competition with XAA (50 μM) in HEPES buffer.

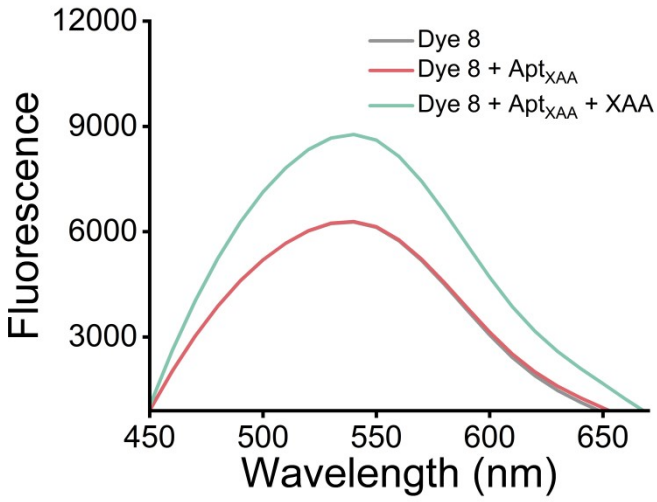

Fig. S11 Fluorescence spectra (λ_{ex} = 410 nm) of S2153 (10 μM) upon binding to Apt_{XAA} (5 μM) and subsequent competition with XAA (50 μM) in HEPES buffer.

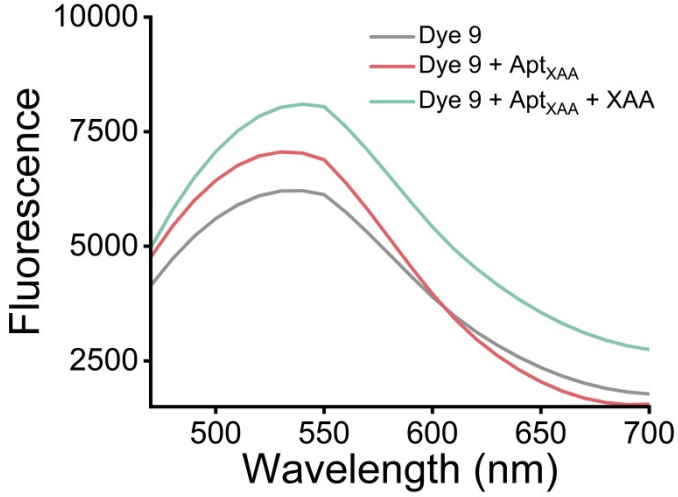

Fig. S12 Fluorescence spectra (λ_{ex} = 430 nm) of 3OUMARIN 525 (10 μM) upon binding to Apt_{XAA} (5 μM) and subsequent competition with XAA (50 μM) in HEPES buffer.

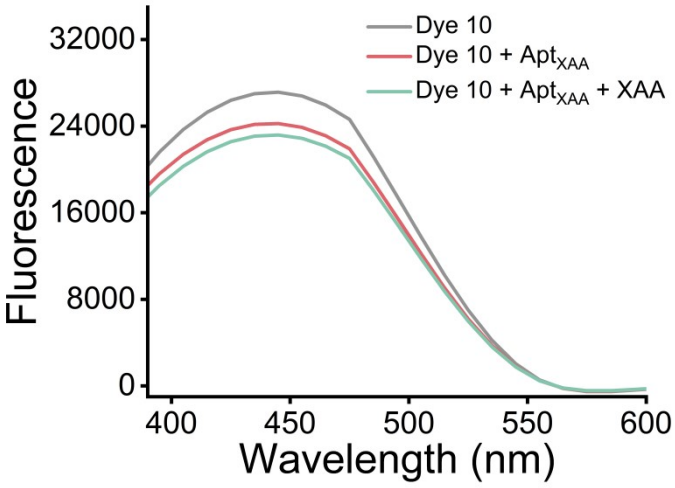

Fig. S13 Fluorescence spectra (λ_{ex} = 345 nm) of Coumarin 478 (10 μM) upon binding to Apt$_{XAA}$ (5 μM) and subsequent competition with XAA (50 μM) in HEPES buffer.

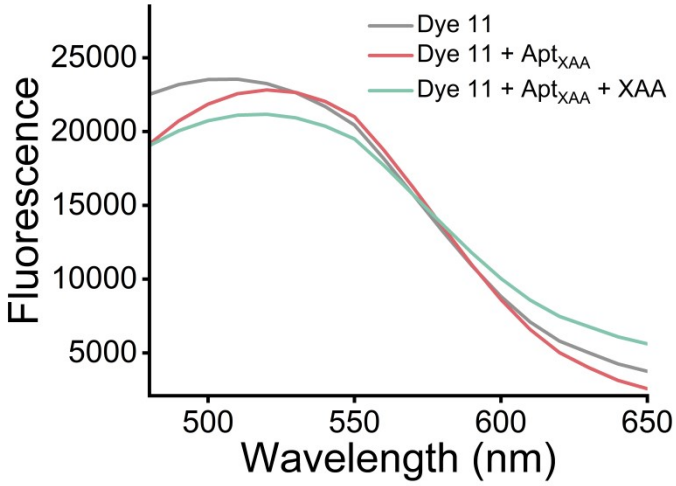

Fig. S14 Fluorescence spectra (λ_{ex} = 450 nm) of Exciton Coumarin 545 (10 μM) upon binding to Apt$_{XAA}$ (5 μM) and subsequent competition with XAA (50 μM) in HEPES buffer.

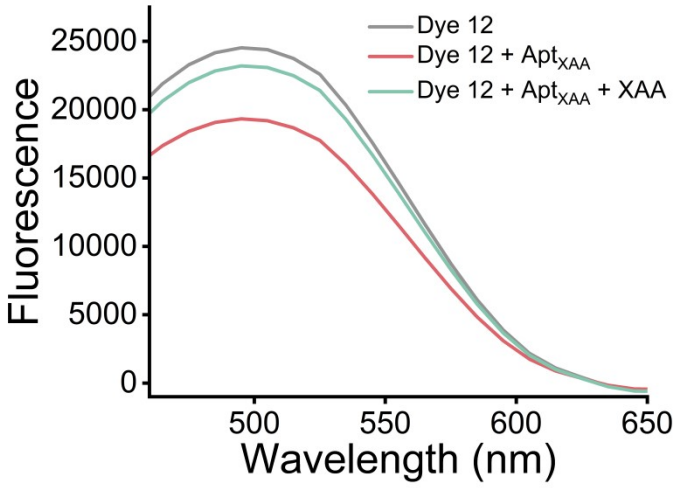

Fig. S15 Fluorescence spectra (λ_{ex} = 415 nm) of Coumarin 30 (10 μM) upon binding to Apt$_{XAA}$ (5 μM) and subsequent competition with XAA (50 μM) in HEPES buffer.

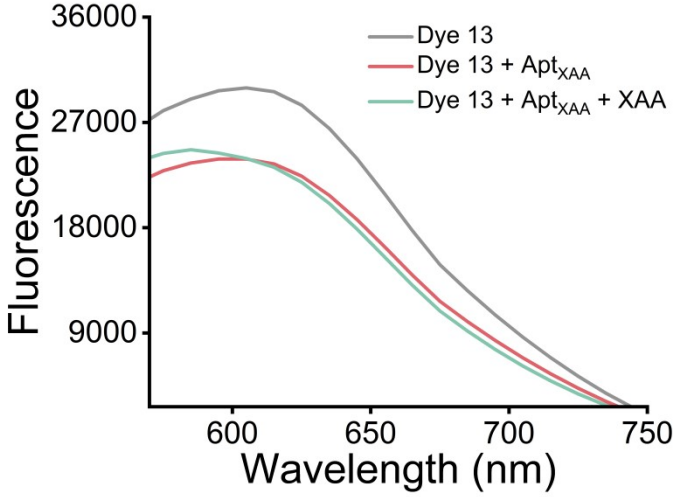

Fig. S16 Fluorescence spectra (λ_{ex} = 475 nm) of Coumarin 545T (10 μM) upon binding to Apt$_{XAA}$ (5 μM) and subsequent competition with XAA (50 μM) in HEPES buffer.

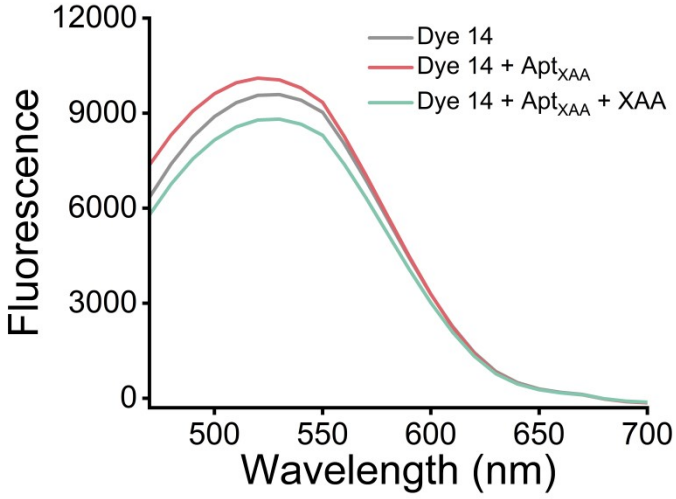

Fig. S17 Fluorescence spectra (λ_{ex} = 430 nm) of Coumarin 510 (10 μM) upon binding to Apt_{XAA} (5 μM) and subsequent competition with XAA (50 μM) in HEPES buffer.

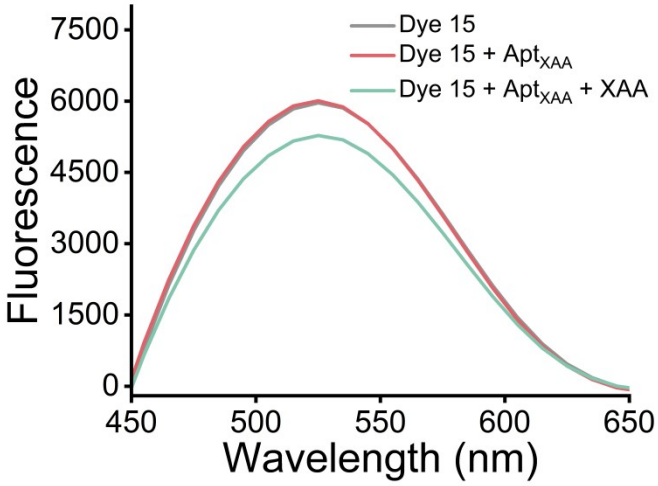

Fig. S18 Fluorescence spectra (λ_{ex} = 405 nm) of Coumarin 73 (10 μM) upon binding to Apt_{XAA} (5 μM) and subsequent competition with XAA (50 μM) in HEPES buffer.

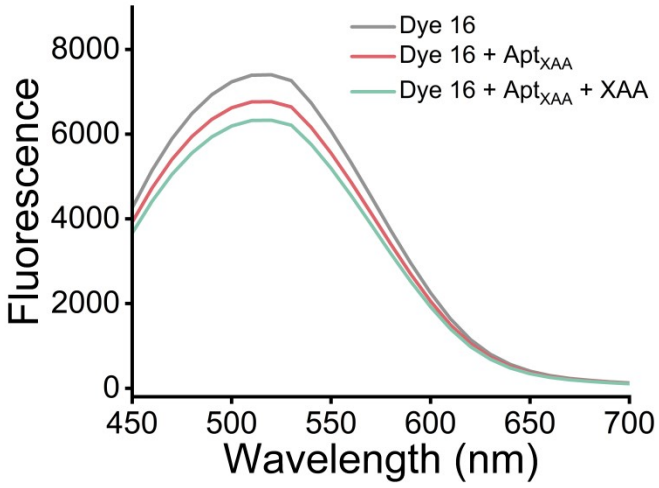

90

91 **Fig. S19** Fluorescence spectra (λ_{ex} = 400 nm) of Coumarin 151 (10 μM) upon binding

92 to Apt$_{XAA}$ (5 μM) and subsequent competition with XAA (50 μM) in HEPES buffer.

93

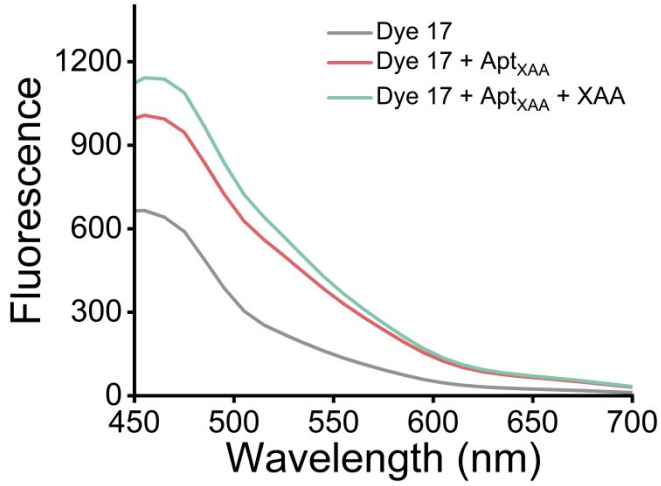

94

95 **Fig. S20** Fluorescence spectra (λ_{ex} = 395 nm) of 3',6'-Dimethoxyfluoran (10 μM) upon

96 binding to Apt$_{XAA}$ (5 μM) and subsequent competition with XAA (50 μM) in HEPES

97 buffer.

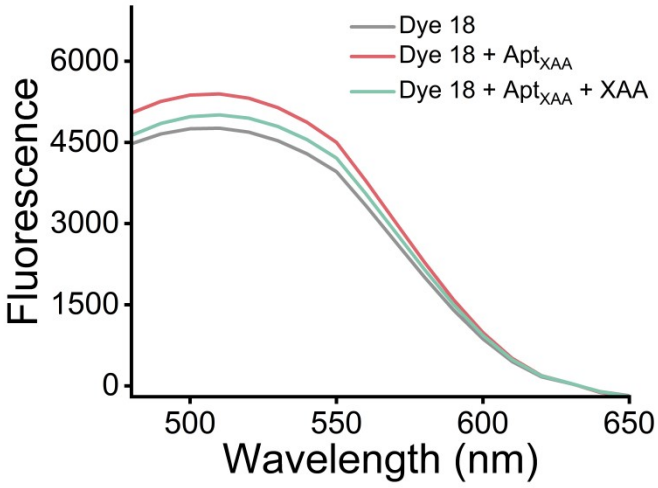

Fig. S21 Fluorescence spectra (λ_{ex} = 440 nm) of Fluorexon (10 μM) upon binding to Apt_{XAA} (5 μM) and subsequent competition with XAA (50 μM) in HEPES buffer.

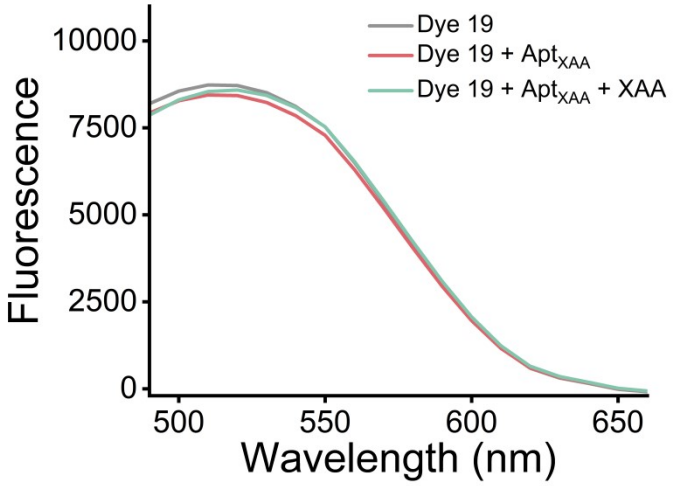

Fig. S22 Fluorescence spectra (λ_{ex} = 450 nm) of 6-Carboxyfluorescein (10 μM) upon binding to Apt_{XAA} (5 μM) and subsequent competition with XAA (50 μM) in HEPES buffer.

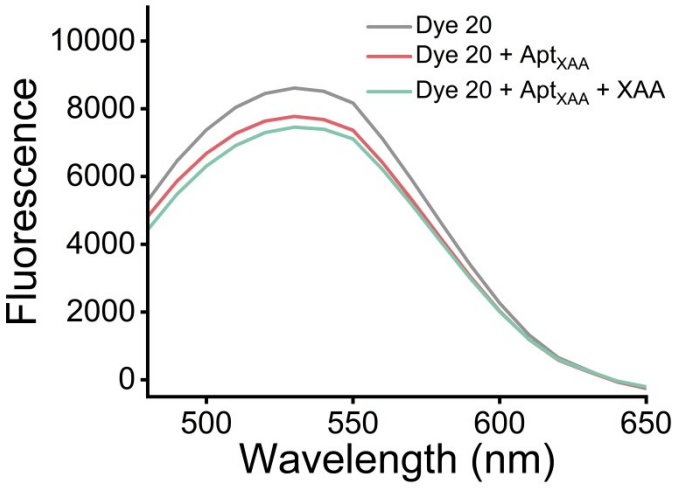

106

107 **Fig. S23** Fluorescence spectra (λ_{ex} = 440 nm) of Fluorescein (10 μM) upon binding to

108 Apt_{XAA} (5 μM) and subsequent competition with XAA (50 μM) in HEPES buffer.

109

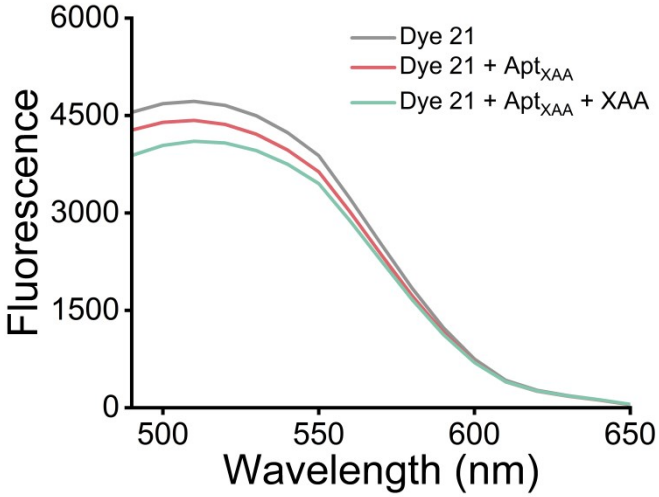

110

111 **Fig. S24** Fluorescence spectra (λ_{ex} = 420 nm) of Fluorescein Sodium (10 μM) upon

112 binding to Apt_{XAA} (5 μM) and subsequent competition with XAA (50 μM) in HEPES

113 buffer.

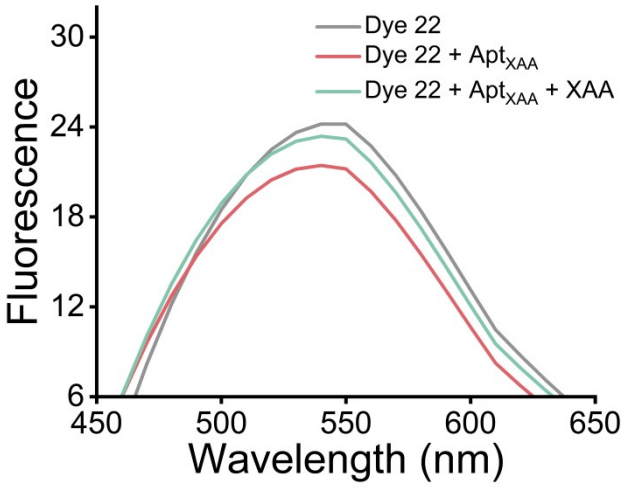

114

115 **Fig. S25** Fluorescence spectra (λ_{ex} = 410 nm) of 3',6'-Dichlorofluoran (10 μM) upon
116 binding to Apt$_{XAA}$ (5 μM) and subsequent competition with XAA (50 μM) in HEPES
117 buffer.

118

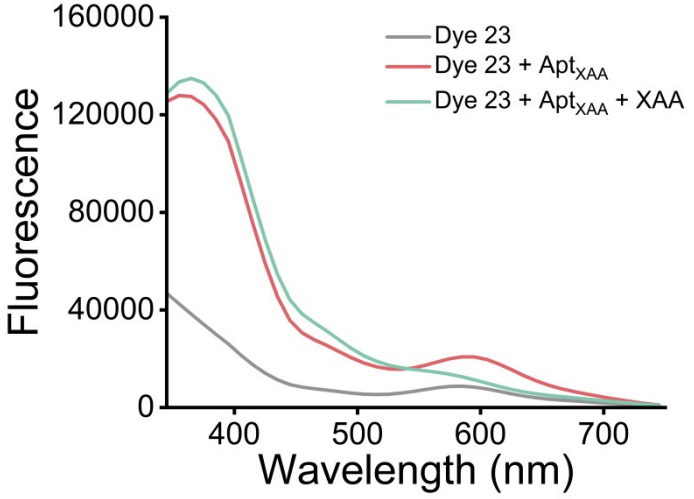

119

120 **Fig. S26** Fluorescence spectra (λ_{ex} = 295 nm) of 2-(2-aminoethyl) Rhodamine B amide
121 (10 μM) upon binding to Apt$_{XAA}$ (5 μM) and subsequent competition with XAA (50
122 μM) in HEPES buffer.

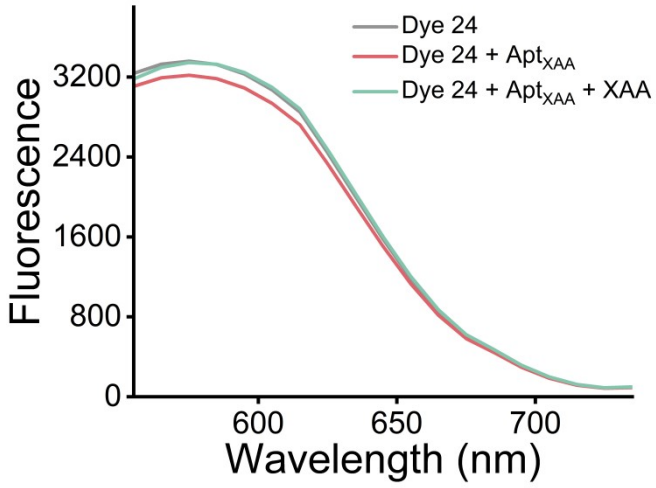

123

124 **Fig. S27** Fluorescence spectra (λ_{ex} = 510 nm) of Sulforhodamine B (10 μM) upon
125 binding to Apt$_{XAA}$ (5 μM) and subsequent competition with XAA (50 μM) in HEPES
126 buffer.

127

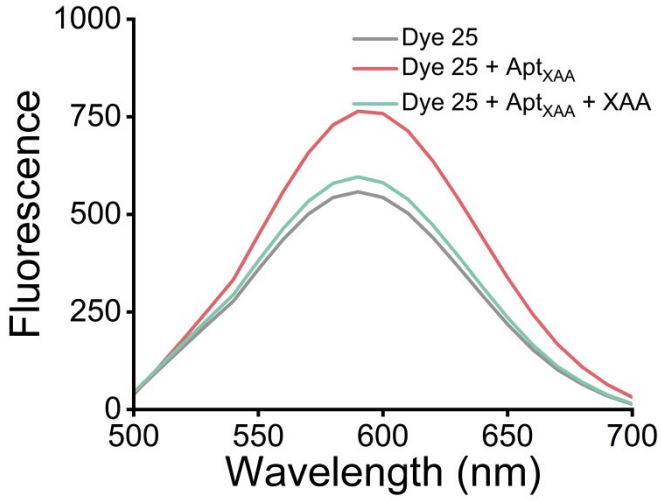

128

129 **Fig. S28** Fluorescence spectra (λ_{ex} = 420 nm) of Rhodamine B (10 μM) upon binding
130 to Apt$_{XAA}$ (5 μM) and subsequent competition with XAA (50 μM) in HEPES buffer.

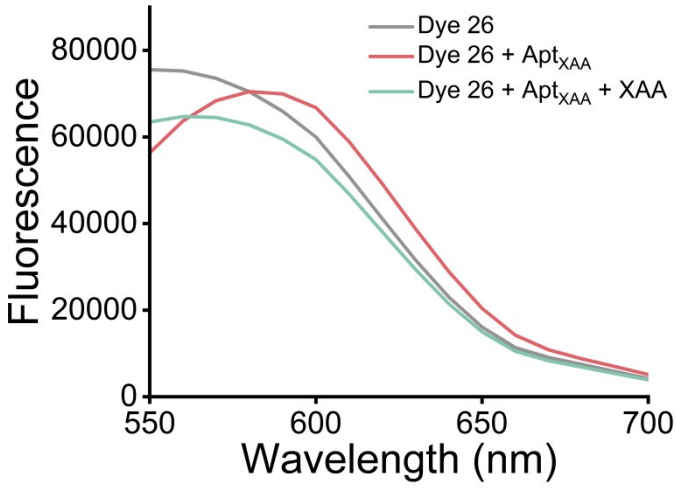

131

132 **Fig. S29** Fluorescence spectra (λ_{ex} = 510 nm) of Pyronin B (10 μM) upon binding to

133 Apt_{XAA} (5 μM) and subsequent competition with XAA (50 μM) in HEPES buffer.

134

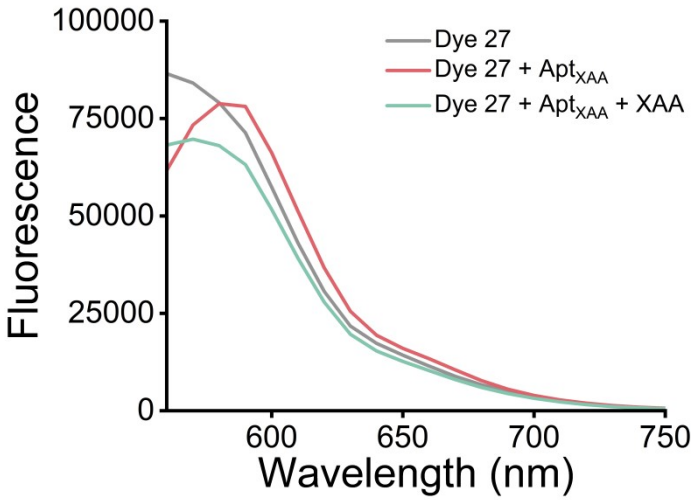

135

136 **Fig. S30** Fluorescence spectra (λ_{ex} = 510 nm) of Pyronin Y (10 μM) upon binding to

137 Apt_{XAA} (5 μM) and subsequent competition with XAA (50 μM) in HEPES buffer.

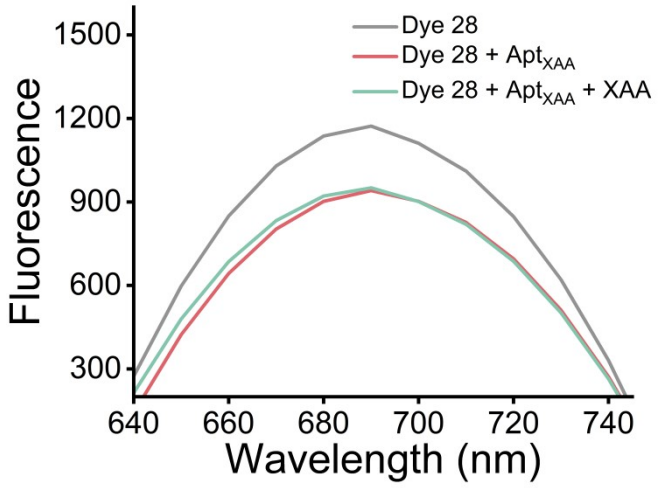

138

139 **Fig. S31** Fluorescence spectra (λ_{ex} = 600 nm) of OXAZINE 1 (10 μM) upon binding to

140 Apt_{XAA} (5 μM) and subsequent competition with XAA (50 μM) in HEPES buffer.

141

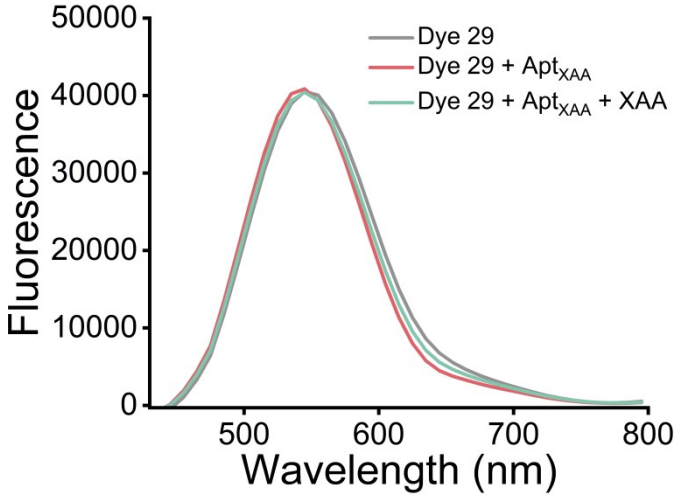

142

143 **Fig. S32** Fluorescence spectra (λ_{ex} = 465 nm) of Basic Orange 14 (10 μM) upon binding

144 to Apt_{XAA} (5 μM) and subsequent competition with XAA (50 μM) in HEPES buffer.

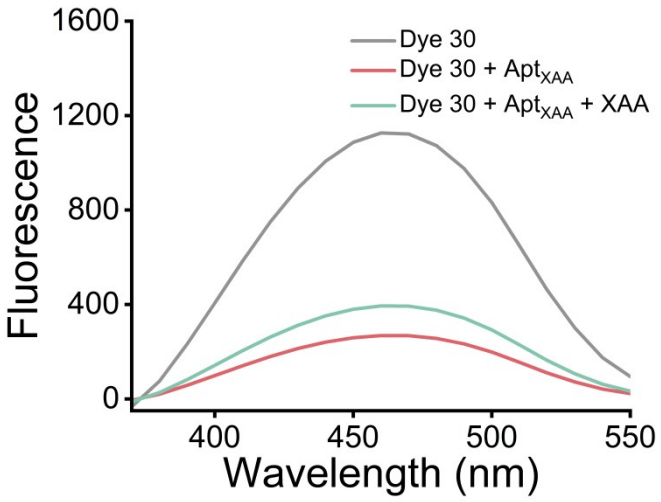

145

146 **Fig. S33** Fluorescence spectra (λ_{ex} = 250 nm) of 9-Aminoacridine (10 μM) upon
147 binding to Apt$_{XAA}$ (5 μM) and subsequent competition with XAA (50 μM) in HEPES
148 buffer.

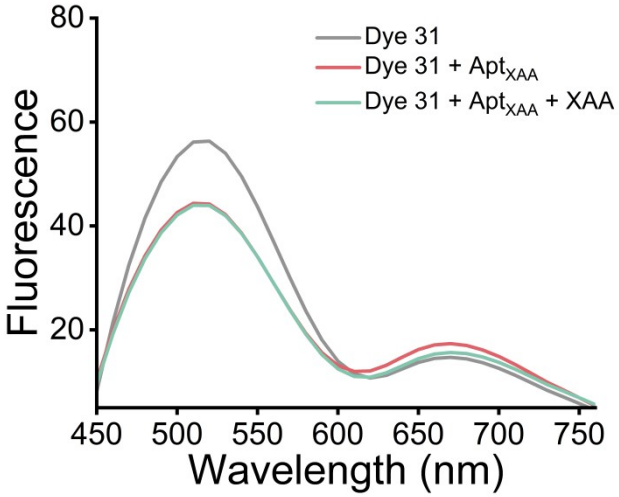

149

150 **Fig. S34** Fluorescence spectra (λ_{ex} = 380 nm) of BODIPY(R) 493/503 (10 μM) upon
151 binding to Apt$_{XAA}$ (5 μM) and subsequent competition with XAA (50 μM) in HEPES
152 buffer.

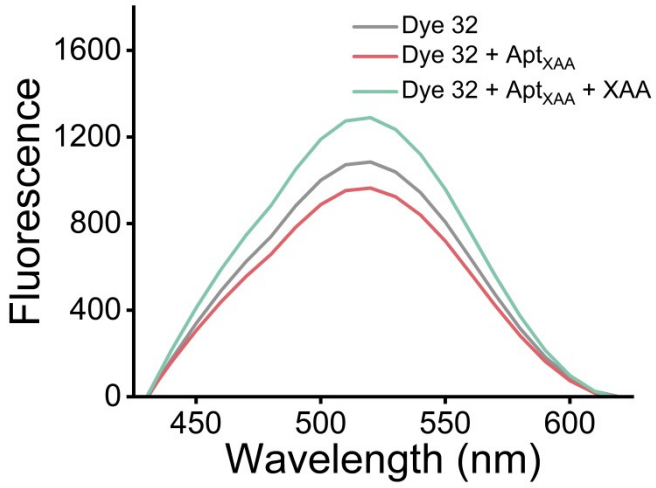

153

154 **Fig. S35** Fluorescence spectra (λ_{ex} = 360 nm) of 8-Phenyl-BODIPY 505/515 (10 μM)
155 upon binding to Apt$_{XAA}$ (5 μM) and subsequent competition with XAA (50 μM) in H
156 EPES buffer.

157

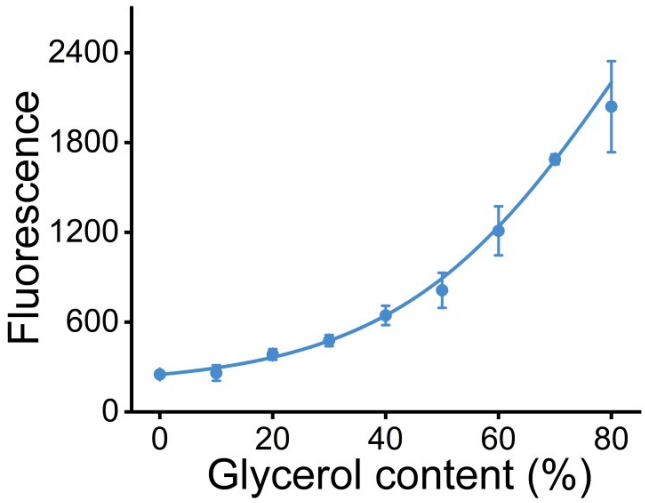

158

159 **Fig. S36** Effect of solvent viscosity on the fluorescence of MV in glycerol/ethylene
160 glycol mixtures.

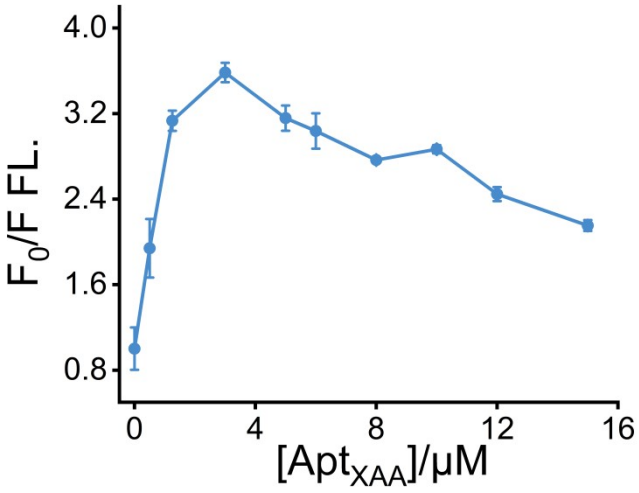

161

162 **Fig. S37** Normalized fluorescence responses of MV complexed with different aptamer

163 concentrations, referenced to signals after addition of XAA.

164

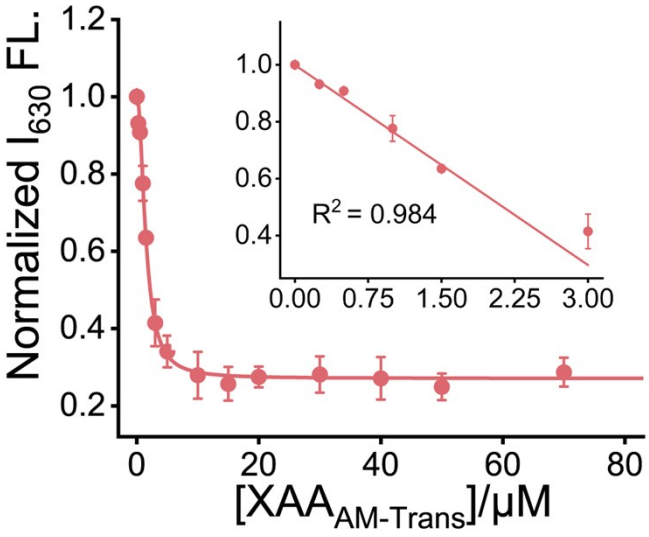

165

166 **Fig. S38** Fluorescence intensity of MV-Apt_{XAA} complexes measured at different XAA_{A}

167 $_{M\text{-}Trans}$ concentrations.

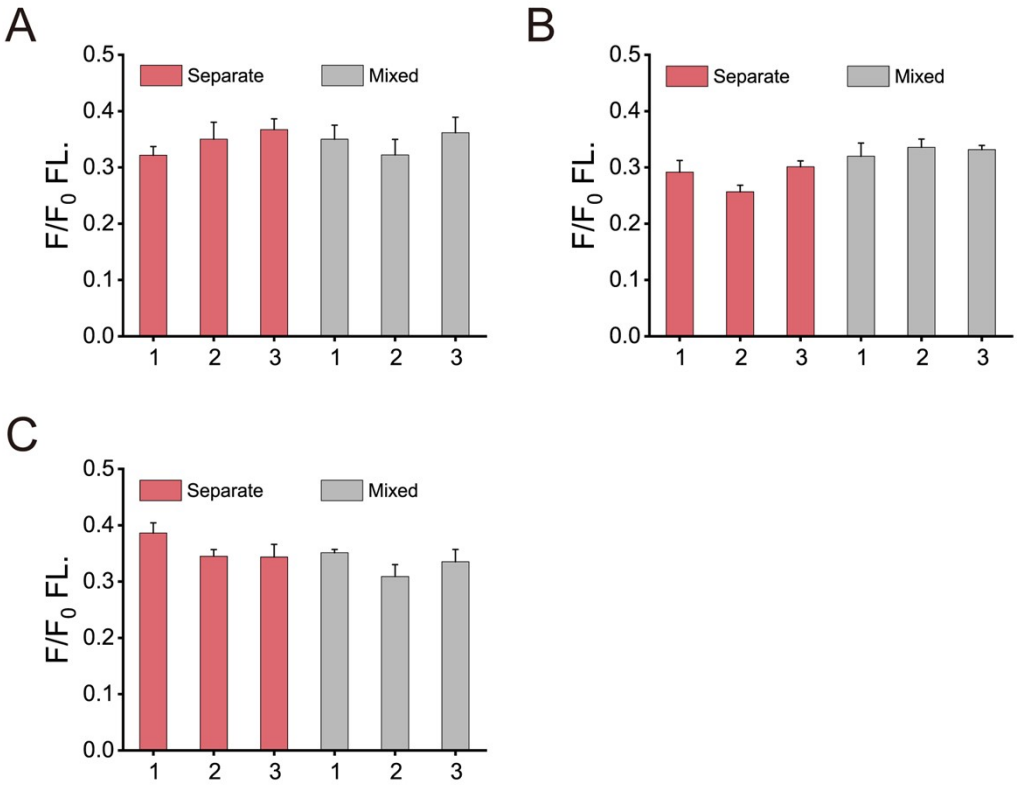

Figure S39. Storage stability of MV, Apt_{XAA}, and the MV- Apt_{XAA} complex for $XAA_{AM\text{-}Trans}$ sensing after storage -20 °C (A), 4 °C (B), and 25 °C (C) for 1, 2 and 3 days. In the "separate" mode, MV and Apt_{XAA} were stored independently and mixed before testing; In the "mixed" mode, the pre-formed complex was stored prior to measurement.

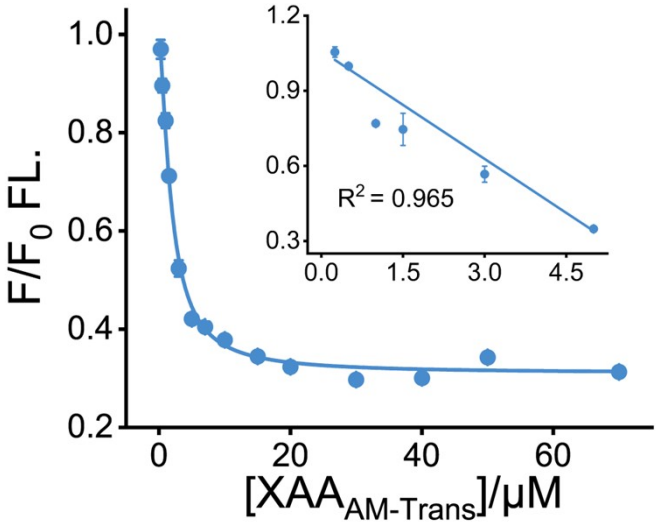

Fig. S40 Fluorescence intensity of MV-Apt_{XAA} complexes measured by POCT platform at different $XAA_{AM\text{-}Trans}$ concentrations.

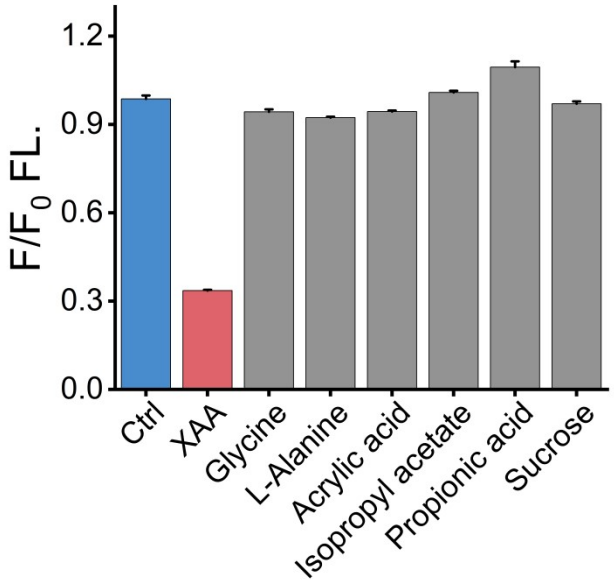

178

179 **Fig. S41** Selectivity of MV-Apt$_{XAA}$ complexes for XAA measured by POCT platform.

180

181 **Table S1**. Summary of existing detection technologies based on aptamers for
182 acrylamide.

Response time	Linear range	Signal response	LOD	Ref.
10 min	1–60 μM	Fluorescence	0.28 μM	Microchem. J. 199 (2024) 110215
70 min	0.05–200 nM	Fluorescence	0.038 nM	Food Chem. 399 (2025) 133938
305 min	0.01–500 nM	Fluorescence	1.802 pM	Food Chem. 493 (2025) 145944
95 min	10nM–0.5 mM	Fluorescence	1.9 nM	J. Agric. Food Chem.70 (2022) 10065-10074.
25.5 min	1–10^5 nM	Fluorescence	1.13nM	Biosens. Bioelectron. 215 (2022) 114581.
50 min	0.01–100 μM	colorimetric	1.53 nM	Anal. Chim. Acta. 1288 (2024) 342150.
50 min	/	SERS	0.326 nM	Spectrochim. Acta A 35 1 (2026) 127322.
30 min	/	Fluorescence /colorimetric	1.00 nM/1.07 nM	J. Hazard. Mater. 466 (2024) 133369.
33 min	0.25-5 μM	Fluorescence	048 μM	This work

183

184

185 **Table S2**. Estimation of $XAA_{AM\text{-}Trans}$ in Potato Chips.

Sample	Added (μM)	Found (μM)	Recovery (%)	RSD (%, n = 3)
Potato Chips（1:20）	0.5	0.55	110.67	9.01
	0.75	0.83	110.04	7.92
	1	0.92	91.78	7.74
	1.5	1.43	95.45	7.04
	2	1.96	98.09	6.71

186